THE JOURNAL OF BIOLOGICAL CHEMISTRY VOL. 282, NO. 16, pp. 12010–12021, April 20, 2007

Pro-apoptotic Activity of Novel Isatin-Schiff Base Copper(II) Complexes Depends on Oxidative Stress Induction and Organelle-selective Damage*[S]

Received for publication, November 27, 2006, and in revised form, February 22, 2007 Published, JBC Papers in Press, February 27, 2007, DOI 10.1074/jbc.M610927200

Giuseppe Filomeni[‡1], Giselle Cerchiaro[§2], Ana Maria Da Costa Ferreira[§], Angelo De Martino[‡], Jens Z. Pedersen[‡], Giuseppe Rotilio[‡], and Maria R. Ciriolo[‡3]

From the [‡]Department of Biology, University of Rome "Tor Vergata," Via della Ricerca Scientifica, 00133 Rome, Italy and the [§]Departamento de Química Fundamental, Instituto de Química, Universidade de São Paulo, P. O. Box 26077, CEP 05513-970 São Paulo, São Paulo, Brazil

We characterized the pro-apoptotic activity of two new synthesized isatin-Schiff base copper(II) complexes, obtained from isatin and 1,3-diaminopropane or 2-(2-aminoethyl)pyridine: (Cu(isapn)) and ($Cu(isaepy)_2$), respectively. We demonstrated that these compounds trigger apoptosis via the mitochondrial pathway. The early induction of the p53/p21 system indicates a role for p53 in cell death, however, experiments carried out with small interfering RNA against p53, or with cells lacking p53, support that a p53-independent mechanism can also occur. The extent of apoptosis mirrors the kinetics of intracellular copper uptake. Particularly, $Cu(isaepy)_2$ enters the cells more efficiently and specifically damages nuclei and mitochondria, as evidenced by atomic absorption analysis of copper content and by the extent of nuclear and mitochondrial integrity. Conversely, Cu(isapn), although less permeable, induces a widespread oxidative stress, as demonstrated by analyses of reactive oxygen species concentration, and oxidation of proteins and lipids. The increase of the antioxidant defense, through the overexpression of Cu,Zn-SOD, partially counteracts cell death; whereas retinoic acid-mediated differentiation completely rescues cells from apoptosis induced by both compounds. The activation of JNK- and Akt-mediated phosphorylative pathways has been found to be not functional for apoptosis induction. On the contrary, apoptosis significantly decreased when the analogous zinc complex was used or when $Cu(isaepy)_2$ was incubated in the presence of a copper chelator. Altogether, our data provide evidence for a dual role of these copper(II) complexes: they are able to vehicle copper into the cell, thus producing reactive oxygen species, and could behave as delocalized lipophilic cation-like molecules, thus specifically targeting organelles.

In the last years synthesis and characterization of novel anti-tumor compounds have represented a field of research that has aroused expectations for more specific and less toxic therapies. Besides DNA and cellular replication, which so far represented the principal targets of cancer treatment, other intracellular compartments and other cell functions, as well as the microenvironment of cancer cells, have become the targets of new and more specific therapies (1–6). For instance, tumor cells are known to show different redox sensitivity or to have low levels of antioxidants, which may lead to an increase of radical species. This phenomenon represents a double-edged sword: on one hand it allows the activation of several redox-sensitive transcription factors inducing tumor proliferation and cell cycle progression (7–10); on the other it can represent an important tool in selectively inducing apoptosis (11–14). Many chemical agents still used in chemotherapy are exploiting this feature; in fact they easily undergo one-electron redox cycling with oxygen, giving rise to superoxide production and oxidative insult. Doxorubicin, daunorubicin, and bleomycin, are among the most used and well known examples of such chemotherapeutics (15–17), but recently particular attention has been addressed also to transition metals, such as copper (18, 19).

Copper is a micronutrient essential for cell survival because it functions as cofactor of several metalloenzymes (*e.g.* Cu,Zn-SOD[4] and cytochrome *c* oxidase), but it is also toxic when present at high concentrations (20). In fact, existing in two redox states, copper(I) and copper(II), it represents an excellent catalyst of redox cycles in the presence of oxygen (21), generating partially reduced and highly reactive O_2 derivatives, the so-called "reactive oxygen species" (ROS). Besides their well known detrimental effects, ROS can also act as second messengers, which, depending on their concentration and the protein

* This work was supported in part by grants from Ministero della Salute, Ministero dell'Università e della Ricerca (to M. R. C.), Fondo per gli Investimenti della Ricerca di Base (FIRB) (to G. R.), and Brazilian agency Fundação de Amparo à Pesquisa do Estado de São Paulo (to A. M. D.). The costs of publication of this article were defrayed in part by the payment of page charges. This article must therefore be hereby marked "*advertisement*" in accordance with 18 U.S.C. Section 1734 solely to indicate this fact.

[S] The on-line version of this article (available at http://www.jbc.org) contains supplemental Figs. S1–S2.

[1] Recipient of fellowship "Santina Grillini" from Italian Association for Cancer Research (AIRC-FIRC).

[2] Recipient of a fellowship from Coordenação de Aperfeiçoamento de Pessoal de Nível Superior (CAPES) while at the University of Rome "Tor Vergata."

[3] To whom correspondence should be addressed. Tel.: 39-06-7259-4369; Fax: 39-06-7259-4311; E-mail: ciriolo@bio.uniroma2.it.

[4] The abbreviations used are: SOD, superoxide dismutase; AIF, apoptosis inducing factor; $Cu(isaepy)_2$, bis-[(2-oxindol-3-yl-imino)-2-(2-aminoethyl)pyridine-*N*,*N*′]copper(II); Cu(isapn), [bis-(2-oxindol-3-yl-imino)-1,3-diaminopropane-*N*,*N*′,*O*,*O*′]copper(II); EPR, electron paramagnetic resonance; JNK, c-Jun N-terminal kinase; PARP, poly(ADP-ribose) polymerase; RA, retinoic acid; ROS, reactive oxygen species; TRIEN, triethylenetetramine; Zn(isaepy), [(2-oxindol-3-yl-imino)-2-(2-aminoethyl)pyridine-*N*,*N*′]zinc(II); zVAD-fmk, benzyloxycarbonyl-Val-Ala-Asp-fluoromethyl ketone; TES,2-{[2-hydroxy-1,1-bis(hydroxymethyl)ethyl]amino}ethanesulfonic acid; PBS, phosphate-buffered saline; siRNA, small interfering RNA.

target involved, can trigger different signal transduction pathways ultimately leading to cell survival or death response (22).

Because the clinical success of cisplatin for the treatment of several tumor cell types has been amply demonstrated, other metal-based compounds have been tested for their anti-tumor activity, to discover more effective and less toxic drugs than cisplatin (23, 24). In this context copper has a long history of medical application, however, its potential anti-tumor properties have been explored only in the last few decades (25). Anti-tumor activity of copper thiosemicarbazone complexes was reported as early as the 1960s (26), however, although many copper-based anti-tumor agents induced cell death *in vitro*, their further use was limited, due to the low water solubility and relatively high toxicity *in vivo* (26–28).

We previously synthesized novel isatin-Schiff base copper(II) complexes and characterized their chemical, physical, and biological properties, suggesting a potential role of some of them in the activation of the apoptotic program in different tumor cell lines (29, 30). In this study, we have investigated the molecular mechanisms underlying the activation of apoptosis upon treatment with two specific isatin-diimine copper(II) complexes: Cu(isapn), and $Cu(isaepy)_2$, in SH-SY5Y neuroblastoma cells, demonstrating that their pro-apoptotic activity involves the mitochondrial pathway. Because of the different copper coordinations characterizing the two complexes, the molecular events upstream of the execution of apoptosis are peculiar of each compound and seem to be tightly associated with the relative kinetics of copper uptake inside the cells.

EXPERIMENTAL PROCEDURES

Materials—Isatin-diimine copper(II) complexes bis-[(2-oxindol-3-yl-imino)-1,3-diaminopropane-*N*,*N*′,*O*,*O*′]copper(II) perchlorate ([Cu(isapn)]$(ClO_4)_2$) and [bis-(2-oxindol-3-yl-imino)-2-(2-aminoethyl)pyridine-*N*,*N*′]copper(II) perchlorate ([$Cu(isaepy)_2$]$(ClO_4)_2$), named here *Cu(isapn)* and *Cu(isaepy)*$_2$, respectively (Fig. 1, *A* and *B*), were synthesized as previously described (30). The analogous isatin-imine zinc(II) complex ([Zn(isaepy)Cl_2]), designated as *Zn(isaepy)*, was prepared similarly using zinc chloride to metallate *in situ* the isaepy ligand (Fig. 1*C*). Dimethyl sulfoxide (Me_2SO), dithiothreitol, EDTA, EGTA, paraformaldehyde, propidium iodide, *tert*-butyl hydroperoxide, sodium orthovanadate, triethylenetetramine (TRIEN), and Triton X-100 were from Sigma. Goat anti-mouse and anti-rabbit IgG (H+L)-horseradish peroxidase conjugate was from Bio-Rad. TES was from U.S. Biological Corp. (Cleveland, OH). All other chemicals were obtained from Merck (Darmstadt, Germany).

Cell Culture—Human neuroblastoma cells SH-SY5Y were purchased from the European Collection of Cell Culture and grown in Dulbecco's modified Eagle's medium, F-12 medium. Promonocytoma U937 were from the American Type Culture Collection; melanoma M14 were kindly provided by Dr. Gabriella Zupi from the Experimental Chemotherapy Laboratory, Regina Elena Cancer Institute of Rome, and grown in RPMI 1640 medium; cervical carcinoma HeLa cells stably transfected with pSUPER vector containing p53 siRNAs (pSUPER-p53), or with empty vector (pSUPER) were a gift of Dr. Anna Maria Biroccio from the Experimental Chemotherapy Laboratory, Regina Elena Cancer Institute of Rome, and grown in Dulbecco's modified Eagle's medium. All cell media were supplemented with 10% fetal calf serum, and the cells were grown at 37 °C in an atmosphere of 5% CO_2 in air. Monoclonal SH-SY5Y cell lines transfected with human wild type Cu,Zn-superoxide dismutase (named *h*SOD) were obtained as previously described (31). During the experiments cells were plated at a density of $4 \times 10^4/cm^2$ (for SH-SY5Y, HeLa and M14) or 2×10^5/ml (for U937), unless otherwise indicated.

Treatments—A 5 mM solution of Cu(isapn), $Cu(isaepy)_2$, or Zn(isaepy) was prepared just before the experiments by dissolving the lyophilized compounds in Me_2SO. Treatments were performed with a concentration of 50 μM at 37 °C in medium supplemented with serum. This concentration was chosen for all the experiments because it gave a substantial degree of apoptosis at the times selected (29). As control, equal volumes of Me_2SO (1%) were added to untreated cells. The pancaspase inhibitor zVAD-fmk (Alexis Biochemicals) was used at a final concentration of 100 μM, preincubated for 1 h before the addition of Cu(isapn) and $Cu(isaepy)_2$, and maintained throughout the experimental time. TRIEN, at a final concentration of 150 μM, was added 3 h before the addition of $Cu(isaepy)_2$ and maintained throughout the experiment. A 5 mM solution of copper sulfate in water was prepared just before the experiments and added to culture media at a concentration of 50 μM. Treatments with the specific c-Jun-N-terminal kinase (JNK) inhibitor, SP600125 (Calbiochem-Novabiochem, La Jolla, CA), and the phosphoinositide 3-kinase/Akt pathway inhibitor wortmannin (Calbiochem-Novabiochem) were performed at concentrations of 10 and 5 μM, respectively, because under our experimental conditions they did not result to be toxic. They were added 30 min before the addition of Cu(isapn) or $Cu(isaepy)_2$ and maintained throughout the experiment. Retinoic acid (RA) was added to culture media at a concentration of 20 μM and maintained for 7 days of culture to allow differentiation of cells, which was monitored by analyzing the increased expression of the differentiation marker, growth-associated protein-43 (GAP-43).

Analysis of Cell Viability and Apoptosis—Adherent (after trypsinization) and detached cells were combined, washed with PBS, and stained with 50 μg/ml propidium iodide prior to analysis by a FACScalibur instrument (BD Biosciences). The percentages of apoptotic cells were evaluated according to Nicoletti *et al.* (32) by calculating peak area of hypodiploid nuclei (sub-G_1). Alternatively, cells were collected and counted after trypan blue staining by optical microscopy using a Thoma chamber.

Cell Fractionation and Protein Extraction—Total protein extracts were obtained by rupturing cells with a 30-min incubation on ice in lysis buffer (50 mM Tris-HCl, pH 7.4, 1 mM EDTA, 1 mM EGTA, 1% Triton X-100, 10 mM NaF, 1 mM sodium orthovanadate) and protease inhibitor mixture (Roche Applied Science, Monza, Italy) and centrifuged at 22,300 × *g* for 20 min at 4 °C. Cell fractions were obtained as previously reported (33). Briefly, cells were incubated in hypotonic medium (10 mM Tris-HCl, pH 7.5, 15 mM $MgCl_2$, 10 mM KCl, and protease inhibitor mixture). After 10 min of incubation on

ice, equal volumes of "mitochondrial" buffer containing 400 mM sucrose, 10 mM TES, 0.1 mM EGTA, and 2 mM dithiothreitol was added, and cells were ruptured by 40 strokes in a glass Dounce. Pellets obtained after centrifugation of lysates at 900 × *g* were considered nuclear-enriched fractions, whereas supernatants further centrifuged at 10,000 × *g* produced a mitochondria-(pellet) and cytosol-enriched fraction (supernatant). For purity determination, total cell extracts and each fraction were analyzed by Western blot against: the α subunit of cytochrome *c* oxidase (Cytox) and the 39-kDa subunit of Complex I (specific for mitochondria); Cu,Zn-SOD (mainly present into the cytosol); and lamin A/C (specific for nuclei) (see supplemental data Fig. S1). For nuclear phospho-H2A.X determination, nuclear extracts were obtained by lysing the cells in nucleus buffer (1 mM K_2HPO_4, pH 6.4, 150 mM NaCl, 14 mM $MgCl_2$, 1 mM EGTA, 0.1 mM dithiothreitol, and 0.3% Triton X-100), and the nuclear fractions obtained were further lysed with lysis buffer.

Western Blot Analyses—Protein extracts were electrophoresed by SDS-PAGE and blotted onto nitrocellulose membrane (Bio-Rad). Polyclonal anti-caspase-9, anti-phospho-p42/44 (Thr^{202}/Tyr^{204}) (Cell Signaling Technology, Beverly, MA), anti-phospho-Akt1/2/3, anti-poly(ADP-ribose) polymerase (PARP), anti-p21, anti-Cu,Zn-SOD (Santa Cruz Biotechnology, Santa Cruz, CA), and monoclonal anti-caspase-3 (clone 3G2), anti-phospho-p38 (Thr^{180}/Tyr^{182}) (Cell Signaling Technology), anti-p53 (clone BP5312), anti-α-tubulin (clone DM1A) (Sigma), anti-lamin A/C (UCS Diagnostics, Rome, Italy), anti-phospho-JNK (G7) (Santa Cruz), anti-phospho-H2A.X (Ser^{139}) (clone JBW301, Upstate Biotechnology, Lake Placid, NY), anti-cytochrome c oxidase (α-subunit), and anti-39-kDa subunit of Complex I (Invitrogen-Molecular Probes) were used as primary antibodies. The specific protein complex, formed upon specific secondary antibody treatment, was identified using a Fluorchem Imaging system (Alpha Innotech, Analitica De Mori, Milano, Italy) after incubation with ChemiGlow chemiluminescence substrate (Alpha Innotech).

Measurement of Glutathione, ROS, and Oxidative Damage—Intracellular reduced (GSH) and oxidized (GSSG) forms of the tripeptide glutathione were assayed upon formation of *S*-carboxymethyl derivatives of free thiols with iodoacetic acid, followed by the conversion of free amino groups to 2,4-dinitrophenyl derivatives by the reaction with 1-fluoro-2,4-dinitrobenzene as previously described (34). Detection of intracellular ROS by 2′,7′-dichlorodihydrofluorescein diacetate (Invitrogen-Molecular Probes), analyses of protein carbonyls content as well as malondialdehyde and 4-hydroxynonenal levels were performed as previously described (35).

Fluorescence Microscopy Analyses—Cells were plated on chamber slides at $6 \times 10^4/cm^2$, fixed with 4% paraformaldehyde, and permeabilized. Afterward, they were washed exhaustively with PBS, blocked with PBS containing 10% fetal calf serum, and incubated with (a) monoclonal anti-cytochrome *c* antibody (clone G742A) (Promega) and polyclonal anti-AIF antibody (Chemicon International, Temecula, CA). Cells were then washed with PBS and probed with an Alexa Fluor®-488 goat anti-mouse and an Alexa Fluor® 568-conjugated goat anti-rabbit secondary antibodies (1:1000) (Invitrogen-Molecular Probes), then analyzed by fluorescence microscopy. (b) Monoclonal anti-Ser^{139}-phosphorylated histone H2A.X antibody, and further probed with an Alexa Fluor®-488 goat anti-mouse secondary antibody (1:1000) (Invitrogen-Molecular Probes). To visualize nuclei, cells were also incubated with propidium iodide solution, washed with PBS, and analyzed by fluorescence microscopy. To evaluate mitochondrial integrity, cells were stained with 50 nM of the mitochondrial transmembrane potential-sensitive probe MitoTracker Red® (Invitrogen-Molecular Probes), washed, and then fixed with 4% paraformaldehyde. To determine the shape of nuclei, cells were also incubated with Hoechst 33342 (1:1000, Calbiochem-Novabiochem), and visualized by fluorescence microscopy. Images of cells were digitized with a Cool Snap video camera connected to Nikon Eclipse TE200 fluorescence microscopy. All images were captured under constant exposure time, gain, and offset.

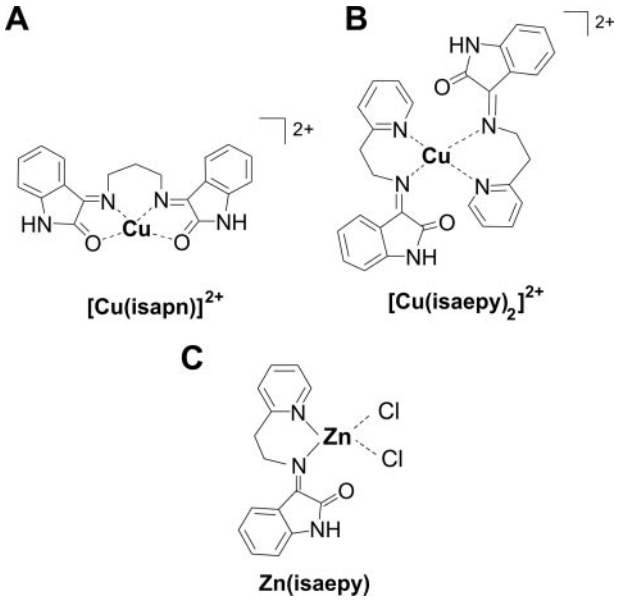

FIGURE 1. **Structures of isatin-Schiff base copper(II) and zinc(II) complexes.** *A*, $[Cu(isapn)]^{2+}$, and *B*, $[Cu(isaepy)_2]^{2+}$. *C*, the analogous isatin-imine zinc(II) complex $[Zn(isaepy)Cl_2]$, designated as *Zn(isaepy)*, was prepared similarly using zinc chloride to metallate *in situ* the isaepy ligand.

Copper Determination—Cell pellets were diluted 1:2 with 65% HNO_3. After 1 week at room temperature, copper concentration was measured by atomic absorption spectrometry using an A Analyst 300 PerkinElmer instrument, equipped with a graphite furnace with platform HGA-800 and an AS-72 auto sampler. Concomitantly, cell media were separated from pellets and analyzed by EPR spectroscopy. EPR spectra were recorded using 80-μl samples in flat glass capillaries (inner cross-section 5 × 0.3 mm) to optimize instrument sensitivity. All measurements were made at 298 K with an ESP300 X-band instrument (Bruker, Karlsruhe, Germany) equipped with a high sensitivity TM_{110}-mode cavity. Spectra were measured over a 1000 G range using 50 milliwatts power, 10 G modulation, and a scan time of 42 s; normally 24 single scans were accumulated to improve the signal to noise ratio.

siRNA Transfections—Twenty-four hours after plating, 50% confluent SH-SY5Y cells were transfected with a 21-nucleotide siRNA duplex directed against the p53 mRNA target sequence,

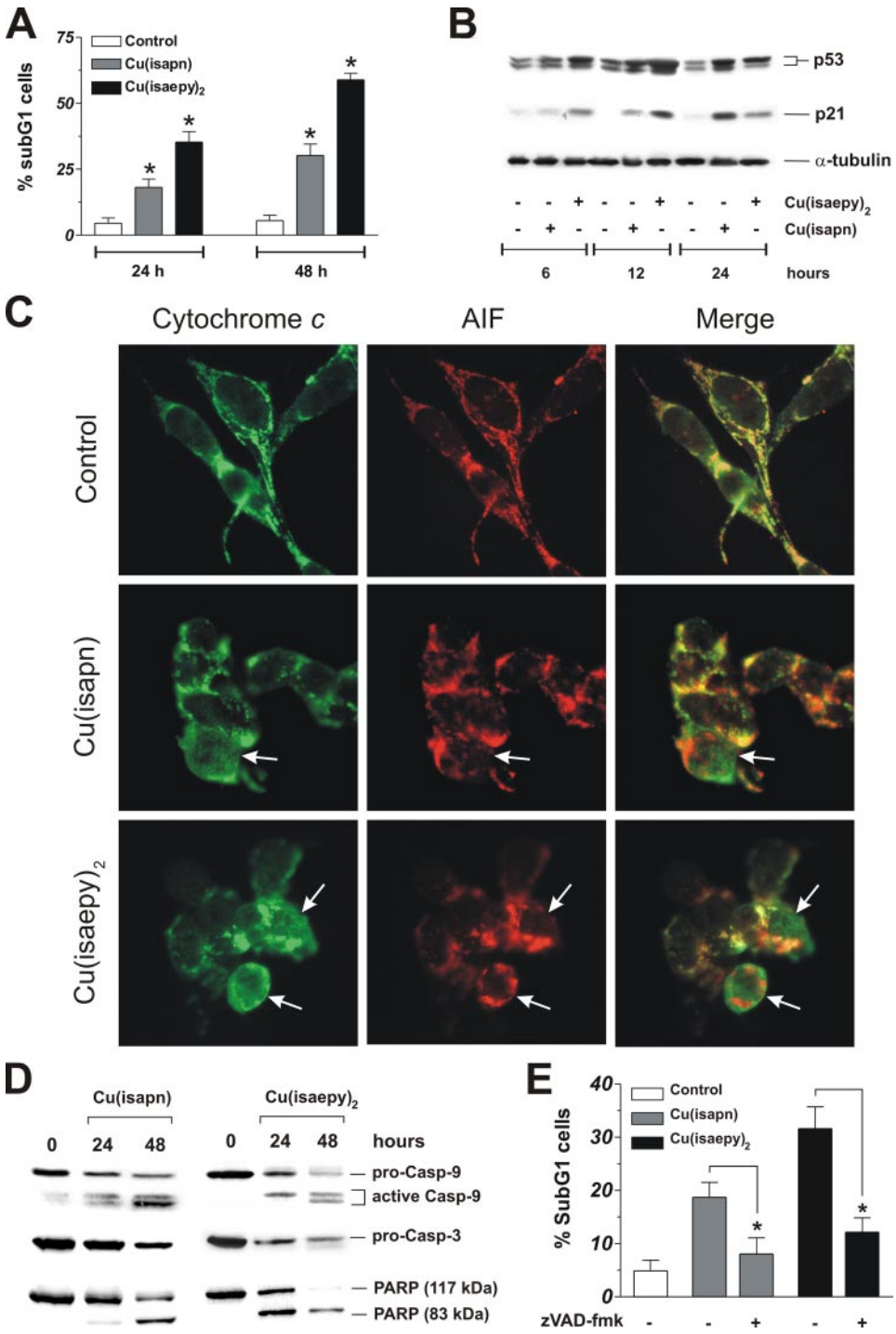

FIGURE 2. **Cu(isapn) and Cu(isaepy)$_2$ induce a p53/p21-associated apoptosis in SH-SY5Y cells via the mitochondrial pathway.** *A*, SH-SY5Y cells were treated with 50 μM Cu(isapn) or Cu(isaepy)$_2$ for 24 and 48 h, washed, and stained with propidium iodide. Analysis of sub-G$_1$ (apoptotic) cells was performed by a FACScalibur instrument and percentages of staining positive cells were calculated using WinMDI version 2.8 software. Data are expressed as mean ± S.D., $n = 12$; *, $p < 0.001$. *B*, SH-SY5Y cells were treated with 50 μM Cu(isapn) or Cu(isaepy)$_2$ for 6, 12, and 24 h. 25 μg of total protein extract was loaded onto each lane for detection of p53 and p21. α-Tubulin was used as loading control. Western blots are from one experiment representative of three that gave similar results. *C*, SH-SY5Y cells were grown on chamber slides, treated for 24 h with 50 μM Cu(isapn) or Cu(isaepy)$_2$, and concomitantly incubated with antibodies anti-AIF (*red*), to visualize mitochondria, and anti-cytochrome *c* (*green*). Images were digitized with a Cool Snap video camera connected to a Nikon Eclipse TE200 fluorescence microscopy. *White arrows* indicate cells where cytochrome *c* was not localized into mitochondria; therefore no superimposition of the two fluorescence was evidenced. *D*, alternatively, SH-SY5Y cells were treated with 50 μM Cu(isapn) or Cu(isaepy)$_2$ for 24 and 48 h. 40 μg of total protein extract was loaded onto each lane for detection of pro- and active caspase-9, pro-caspase 3 and PARP. Western blots are from one experiment representative of three that gave similar results. *E*, SH-SY5Y cells were incubated for 1 h with or without 100 μM pancaspase inhibitor zVAD-fmk, treated with 50 μM Cu(isapn) or Cu(isaepy)$_2$ for 24, washed, and stained with propidium iodide. Analysis of sub-G$_1$ (apoptotic) cells was performed by a FACScalibur instrument and percentages of staining positive cells were calculated using WinMDI version 2.8 software. Data are expressed as mean ± S.D., $n = 5$; *, $p < 0.001$.

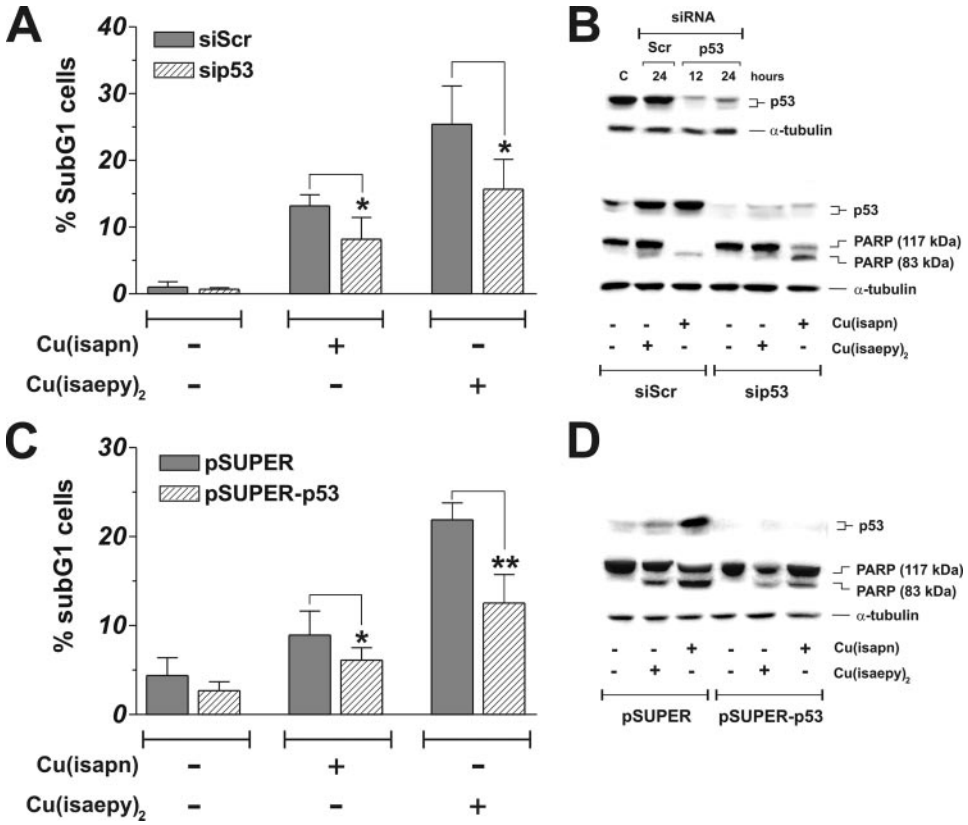

FIGURE 3. **p53 RNA interference partially counteracts apoptosis induced by Cu(isapn) and Cu(isaepy)$_2$.** *A*, SH-SY5Y cells were transiently transfected with siRNA duplex directed against the p53 mRNA target sequence (sip53) or with a scramble siRNA duplex, which does not present homology with any other human mRNAs (siScr). Cell adhesion has been allowed for 9 h, then the cells were treated with 50 μM Cu(isapn) or Cu(isaepy)$_2$ for the next 24, washed, and stained with propidium iodide. Analysis of sub-G$_1$ (apoptotic) cells was performed by a FACScalibur instrument and percentages of staining positive cells were calculated using WinMDI version 2.8 software. Data are expressed as mean ± S.D., $n = 6$; *, $p < 0.05$. *B*, to evaluate the degree of p53 decrease, at the time points indicated, sip53 or siScr cells were harvested and lysed. 25 μg of total protein extract was loaded onto each lane for detection of p53. α-Tubulin was used as loading control. After 9 h from transfection with siScr or sip53, SH-SY5Y cells were then treated with 50 μM Cu(isapn) or Cu(isaepy)$_2$ for 24 h. 40 μg of total protein extract was loaded onto each lane for detection of p53 and PARP. α-Tubulin was used as loading control. Western blots are from one experiment representative of three that gave similar results. *C*, HeLa cells, stably transfected with a pSUPER vector containing p53 siRNA (*pSUPER-p53*) or with empty vector (*pSUPER*) were treated with 50 μM Cu(isapn) or Cu(isaepy)$_2$ for 24 h, washed, and stained with propidium iodide. Analysis of sub-G$_1$ (apoptotic) cells was performed by a FACScalibur instrument and percentages of staining positive cells were calculated using WinMDI version 2.8 software. Data are expressed as mean ± S.D., $n = 6$; *, $p < 0.05$. *D*, pSUPER and pSUPER-p53 cells were treated with 50 μM Cu(isapn) or Cu(isaepy)$_2$ for 24 h. 40 μg of total protein extract was loaded onto each lane for detection of p53 and PARP. α-Tubulin was used as loading control. Western blots are from one experiment representative of three that gave similar results.

5′-GACUCCAGUGGUAAUCUACTT-3′ (sip53) (MWG Biotech, Ebersberg, Germany). Control cells were transfected with a scramble siRNA duplex, which does not present homology with any other human mRNAs (siScr). Cells were transfected by electroporation using a Gene Pulser Xcell system (Bio-Rad) according to the manufacturer's instructions and immediately seeded into fresh medium. Transfection efficiency of siRNA into SH-SY5Y cells was estimated by co-transfecting p53 siRNA with nonspecific rhodamine-conjugated oligonucleotides and found to be >80%.

Protein Determination—Proteins were determined by the method of Lowry *et al.* (36).

Data Presentation—All experiments were done at least five different times unless otherwise indicated. Data were expressed as mean ± S.D. and significance was assessed by Student's *t* test corrected by Bonferroni's method. Differences with p values <0.05 were considered significant.

RESULTS AND DISCUSSION

Cu(isapn) and Cu(isaepy)$_2$ Induce Cell Cycle Arrest and Caspase-dependent Apoptosis—To dissect the mechanisms by which isatin-Shiff base copper(II) complexes induce cell death in tumor cell lines, on the basis of the results previously obtained (29), we selected the most effective molecules, Cu(isapn) and Cu(isaepy)$_2$ (Fig. 1, *A* and *B*), and used them at a concentration of 50 μM. Fig. 2*A* shows representative histograms from cytofluorimetric analyses of SH-SY5Y cells treated with Cu(isapn) and Cu(isaepy)$_2$ for 24 and 48 h, where a more effective increase in the apoptotic cells with Cu(isaepy)$_2$ treatment was evidenced (Fig. 2*A*). Western blot analyses of p53 and p21 showed a strong activation of these two proteins although with different kinetics: rapid for Cu(isaepy)$_2$ and more gradual for Cu(isapn) with a peak of induction at 12 and 24 h, respectively (Fig. 2*B*), indicating that the p53/p21 pathway is activated as response to cell damage. The typical mitochondrial localization of the apoptosis inducing factor (AIF) and endonuclease G showed that no "caspase-independent" mechanism was operative under our experimental conditions (data not shown); searching for the mechanism underlying apoptotic induction, we therefore used the anti-AIF antibody to probe mitochondria. As evidenced by immunofluorescence analyses of SH-SY5Y cells treated for 24 h with copper complexes, AIF fluorescence did not superimpose cytochrome *c* staining (Fig. 2*C*), indicating that cytochrome *c* was efficiently released from mitochondria into the cytosol, and that the intrinsic mitochondrial pathway was operative under our experimental conditions. Concomitantly, Western blot analyses of pro- and active caspase-9, as well as pro-caspase-3 and PARP indicated that each step of the apoptotic program was executed upon treatment with either Cu(isapn) or Cu(isaepy)$_2$ (Fig. 2*D*). In fact, immunoreactive bands of proteolyzed caspase-9 and PARP, together with a significant decrease of pro-caspase-3 were already detected after 24 h of treatment. As final evidence that a caspase-dependent apoptotic response occurred after treatment with both copper complexes, we preincubated the cells with 100 μM of the pan-

caspase inhibitor zVAD-fmk for 1 h and then added Cu(isapn) or $Cu(isaepy)_2$. Fig. 2*E* shows that a recovery of cell viability resulted from the inhibition of caspases activation upon treatment with both compounds, confirming that caspase-mediated apoptosis is the principal mechanism for cell death induction in our experimental system.

To evaluate the role of p53 in apoptosis induction, we transfected SH-SY5Y cells with siRNA against p53 (sip53) or with a scramble sequence that does not present homology with any other human mRNAs (siScr). Western blot analyses of p53 levels indicated that the concentration of the protein rapidly decreased after transfection (see Fig. 3*B*, *upper panel*). Therefore, we decided to treat the cells with Cu(isapn) or $Cu(isaepy)_2$ after 9 h from transfection, time that allowed the cells adhering to the flask and p53 interference being still in progress. Cytofluorimetric analyses show that sip53 cells were significantly resistant to apoptosis if compared with siScr (Fig. 3*A*). This was also confirmed by Western blot of PARP that indicated a more efficient cleavage of the protein occurring in siScr than in sip53 cells (Fig. 3*B*, *bottom panel*). We also performed experiments on HeLa cells stably transfected with a pSUPER vector containing siRNAs for p53 (pSUPER-p53) or with an empty vector (pSUPER). Fig. 3*C* shows cytofluorimetric analyses of apoptosis upon 24 h treatment with Cu(isapn) or $Cu(isaepy)_2$. As previously observed for SH-SY5Y, also for HeLa, the percentage of sub-G_1 cells was significantly reduced upon p53 interference. This result was further confirmed by Western blot analyses of PARP (Fig. 3*D*), suggesting that p53 activation contributes to copper complex-mediated apoptosis. Nevertheless, a considerable amount of p53-independent apoptosis was also observed.

Cu(isapn) and $Cu(isaepy)_2$ Cross the Cell Membrane and Selectively Induce Oxidative Stress—To characterize the capability of Cu(isapn) and $Cu(isaepy)_2$ to enter the cells and the kinetics of their accumulation, we followed copper uptake by atomic absorption analyses. Fig. 4*A* shows that treatments with both compounds resulted in a rapid increase of intracellular copper content that reached a plateau after 12 h. This result was particularly significant, especially when compared with that obtained with copper sulfate, used as control of cellular incorporation of the metal ion. $Cu(isaepy)_2$ seems to be more efficiently incorporated within the cells with respect to Cu(isapn). These results demonstrated a direct relationship between copper uptake and the extent of apoptosis, with $Cu(isaepy)_2$ being more permeating and more efficient in inducing cell death than Cu(isapn). Because the molecules we have synthesized have characteristic EPR spectra (23), we measured the extracellular concentration of $Cu(isaepy)_2$ by EPR spectroscopy. Fig. 4*B* reports the spectra of $Cu(isaepy)_2$ in cell culture media and its relative concentration up to 12 h of treatment. The data suggest that a decrease in the content of copper complex, most probably due to its uptake by cells, was operative under our experimental conditions. Moreover, these results also suggested that the complex was chemically stable during the experimental times selected, as no changes of the EPR parameters were evidenced. To further confirm both hypotheses, we performed the same experiments at 4 °C, a temperature at which metabolic processes are strongly reduced. Fig. 4*C* show that, under these experimental conditions, no significant difference in the extracellular concentration of $Cu(isaepy)_2$ was evidenced. The same results were achieved with Cu(isapn), for which, however, a slower uptake was observed (data not shown), confirming that the decrease of EPR signals measured in cell media after treatment was due to cell uptake of both complexes rather than their stability (see Fig. S2 to compare the different time courses of $Cu(isaepy)_2$ uptake at 37 and 4 °C).

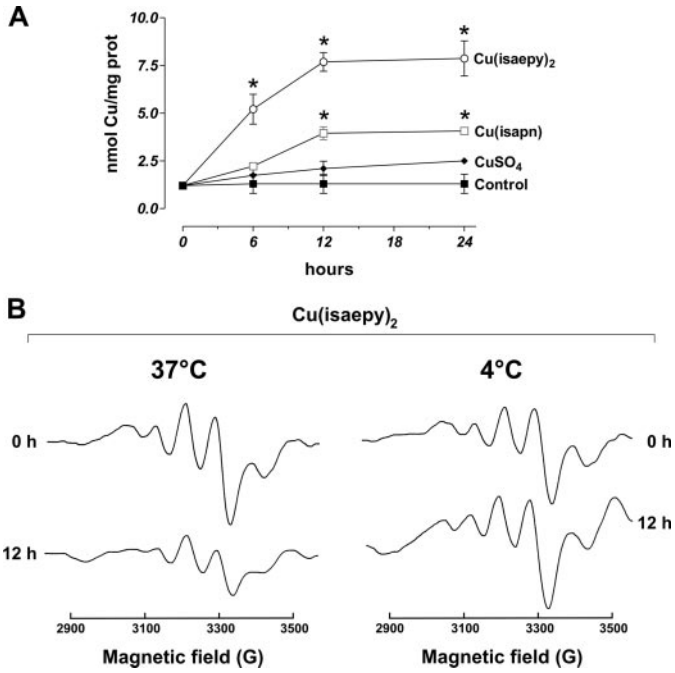

FIGURE 4. **Cu(isapn) and $Cu(isaepy)_2$ induce intracellular copper uptake.** *A*, SH-SY5Y cells were treated with 50 μM Cu(isapn) or $Cu(isaepy)_2$ for 6, 12, and 24 h, exhaustively washed with PBS containing 1 mM EDTA to avoid contamination of extracellularly membrane-bound copper, diluted 1:2 with 65% HNO_3, and analyzed for copper content by atomic absorption. 50 μM copper sulfate ($CuSO_4$) was used as control of copper uptake. Data are expressed as nanomole of copper/mg of total protein and represent the mean ± S.D., $n = 5$; *, $p < 0.001$. *B*, SH-SY5Y cells were treated with 50 μM $Cu(isaepy)_2$ for 12 h at 4 and 37 °C. Cell media were harvested, centrifuged to remove detached cells, and analyzed by EPR technique to measure the copper complex content.

Copper could behave as pro-oxidant by catalyzing intracellular redox cycles with oxygen thus generating free radicals. By spin trapping EPR experiments, using 5,5-dimethyl-1-pyrroline *N*-oxide as the spin scavenger, we previously reported that both Cu(isapn) and $Cu(isaepy)_2$ are able to produce ROS in the presence of hydrogen peroxide, with the former more efficient than the latter in generating 5,5-dimethyl-1-pyrroline *N*-oxide-OH$^{\bullet}$ adducts (29). To determine whether they were still able to generate ROS in a cell system, we measured ROS content by staining SH-SY5Y cells with 2′,7′-dichlorodihydrofluorescein diacetate. Cytofluorimetric analyses shown in Fig. 5*A* demonstrate that Cu(isapn) and $Cu(isaepy)_2$ were pro-oxidants, as ROS production increased with respect to untreated cells. In particular, Cu(isapn) was more effective as an upstream ROS inducer, because the increase of fluorescence was detectable as early as 3 h after treatment. On the other hand, $Cu(isaepy)_2$ did not affect ROS production up to 24 h, the time corresponding to an increased rate of apoptotic cells, allowing us to suggest that this phenomenon could be a downstream event of the death process. Moreover, Cu(isapn)-induced transient damages to both proteins (Fig. 5*B*) and lipids (Fig. 5*C*), as determined by West-

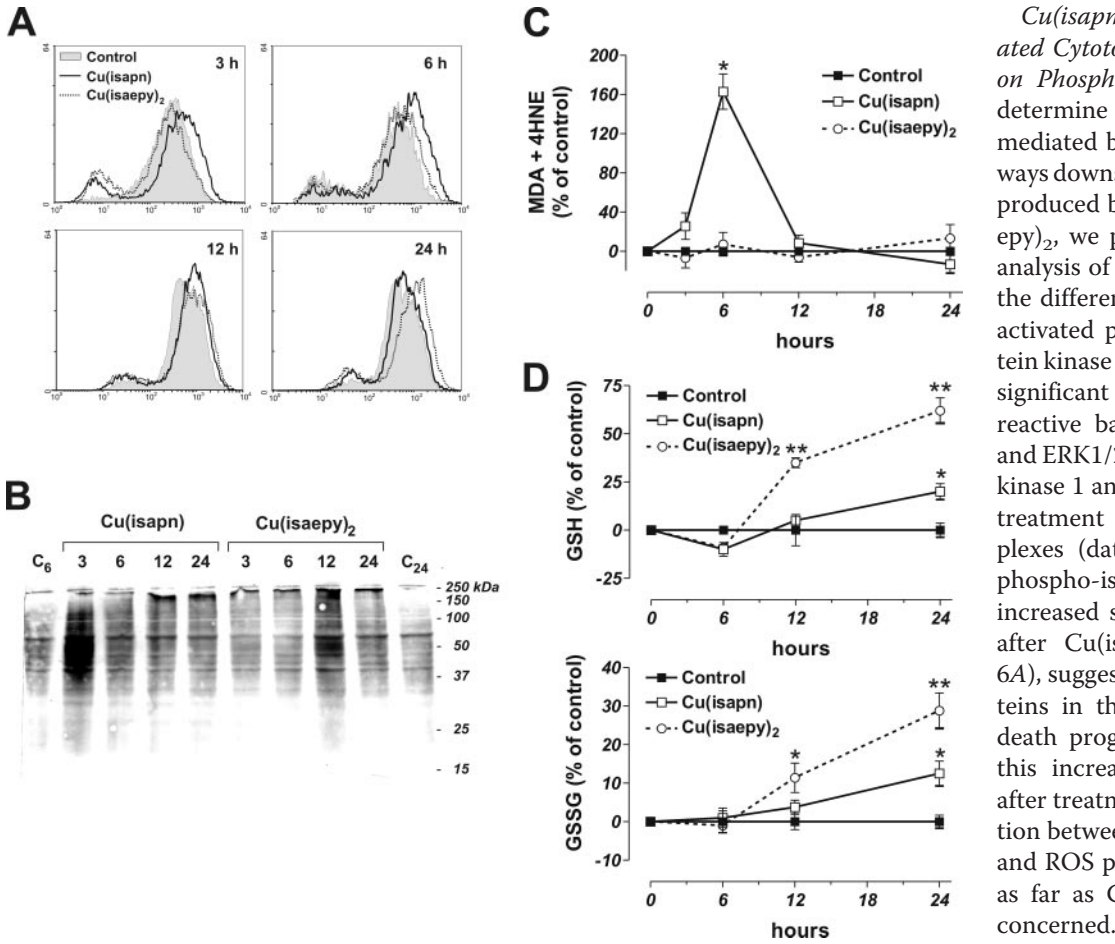

FIGURE 5. **Cu(isapn) and Cu(isaepy)$_2$ induce oxidative stress.** *A*, SH-SY5Y cells were treated with 50 μM Cu(isapn) or Cu(isaepy)$_2$ for 3, 6, 12, and 24 h, and incubated with 50 μM DCF-DA at 37 °C. At the indicated time points, cells were washed with PBS and ROS production was analyzed by a FACScalibur instrument. Histograms shown are representative of three experiments that gave similar results. *B*, at the same time points protein carbonyls were identified upon derivatization with dinitrophenylhydrazine followed by immunoblot using anti-dinitrophenylhydrazine antibody. 20 μg of derivatized proteins were loaded onto each lane. A representative Western blot of three that gave similar results is shown. *C*, alternatively lipid peroxidation was evaluated by measuring the levels of malondialdehyde and 4-hydroxynonenal using a colorimetric method. Data are expressed as % of control and represent the mean ± S.D., $n = 5$; *, $p < 0.001$. *D*, SH-SY5Y cells were treated with 50 μM Cu(isapn) or Cu(isaepy)$_2$ for 6, 12, and 24 h, exhaustively washed with PBS containing 1 mM EDTA, to avoid glutathione oxidation, and used for high performance liquid chromatography determination of intracellular GSH and GSSG. Data are expressed as % of control and represent the mean ± S.D., $n = 5$; *, $p < 0.05$; **, $p < 0.001$.

ern blot of carbonyls and colorimetric analyses of lipid peroxidation by products, respectively. Interestingly, the major capability of this compound in generating ROS was in accordance with the occurrence of an earlier appearance of protein carbonyls as well as malondialdehyde and 4-hydroxynonenal (3–6 h after treatment). In contrast, Cu(isaepy)$_2$ treatment resulted in a later oxidative protein damage (12 h) without compromising lipid structures.

We measured the concentration and the redox state of glutathione, as this molecule represents the most important low molecular weight antioxidant, particularly involved in ROS scavenging and xenobiotic detoxification. Fig. 5*D* shows that, after 6 h of treatment with Cu(isapn) and Cu(isaepy)$_2$, both GSH and GSSG increased with an extent mirroring the kinetics of copper uptake, suggesting that the levels of glutathione, due to its ability to bind copper and detoxify xenobiotics, might be coupled with the intracellular content of copper compounds.

Cu(isapn) and Cu(isaepy)$_2$-mediated Cytotoxicity Does Not Depend on Phosphorylative Pathways—To determine whether apoptosis was mediated by phosphorylative pathways downstream of oxidative stress produced by Cu(isapn) and Cu(isaepy)$_2$, we performed Western blot analysis of phospho-active levels of the different members of mitogen-activated protein kinases and protein kinase B, also known as Akt. No significant changes in the immunoreactive bands of active p38^{MAPK} and ERK1/2 (extracellular regulated kinase 1 and 2) were detected upon treatment with the copper complexes (data not shown), but the phospho-isoforms of JNK and Akt increased significantly, particularly after Cu(isaepy)$_2$ treatment (Fig. 6*A*), suggesting a role for these proteins in the induction of the cell death program. However, because this increase occurred very early after treatment (3–6 h), no correlation between Akt or JNK activation and ROS production can be stated, as far as Cu(isaepy)$_2$ treatment is concerned. To determine the role of Akt in cell response to Cu(isapn) and Cu(isaepy)$_2$, we preincubated SH-SY5Y cells with wortmannin, a specific inhibitor of the Akt upstream kinase phosphoinositide 3-kinase, and then treated the cells with the copper complexes. Fig. 6*B* shows that inhibition of Akt before treatment with Cu(isapn) and Cu(isaepy)$_2$ resulted in a significant increase of sub-G_1 cell population. Western blot analyses of cell lysates confirmed that wortmannin incubation produced blockage of the Akt-mediated pathway (Fig. 6*C*) and concomitantly showed no effect on the phospho-active form of JNK after Cu(isapn) and Cu(isaepy)$_2$ treatments, suggesting that Akt and JNK activation are independent responses. Preincubation with the specific JNK pathway inhibitor SP600125 did not result in modified cell survival to treatments with either Cu(isapn) or Cu(isaepy)$_2$ (Fig. 6*D*), indicating that JNK activation could represent just an epiphenomenon of the copper complex-induced cytotoxicity, which does not directly relate to the apoptotic process.

Increase of Antioxidant Defense or Differentiation by Retinoic Acid Rescues SH-SY5Y Cells from Cu(isapn) and Cu(isaepy)$_2$-induced Cytotoxicity—The results so far presented indicate a different time dependence and occurrence of the oxidative markers upon treatments with Cu(isapn) or Cu(isaepy)$_2$, which could reflect the different structures of the copper

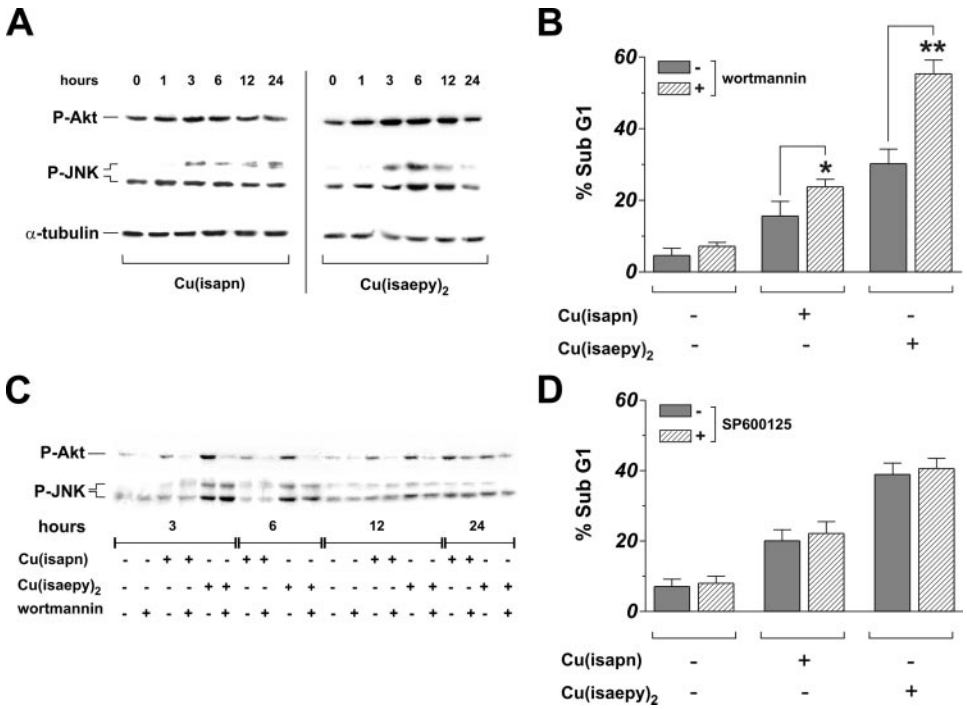

FIGURE 6. **JNK and Akt are not involved in Cu(isapn) and Cu(isaepy)$_2$-induced apoptosis.** *A*, SH-SY5Y cells were treated with 50 μM Cu(isapn) or Cu(isaepy)$_2$ up to 24 h. 20 μg of total protein extract was loaded onto each lane for detection of phosphorylated forms of JNK (*P-JNK*) and Akt (*P-Akt*). α-Tubulin was used as loading control. Western blots are from one experiment representative experiment of three that gave similar results. *B*, SH-SY5Y cells were treated with 50 μM Cu(isapn) or Cu(isaepy)$_2$ for 24 h previous to a 1-h incubation with the phosphoinositide 3-kinase/Akt pathway inhibitor, wortmannin. Cells were washed and stained with propidium iodide. Analysis of sub-G$_1$ (apoptotic) cells was performed by a FACScalibur instrument and percentages of staining positive cells were calculated using WinMDI version 2.8 software. Data are expressed as mean $\pm$ S.D., $n = 5$; *, $p < 0.05$; **, $p < 0.001$. *C*, alternatively 20 μg of total protein extract was loaded onto each lane and used for the detection of phosphorylated forms of JNK (*P-JNK*) and Akt (*P-Akt*). Western blots are from one experiment representative of three that gave similar results. *D*, SH-SY5Y cells were treated with 50 μM Cu(isapn) or Cu(isaepy)$_2$ for 24 h previous to a 1-h incubation with the specific JNK inhibitor, SP600125. Cells were washed and stained with propidium iodide. Analyses of sub-G$_1$ (apoptotic) cells was performed by a FACScalibur instrument and percentages of staining positive cells were calculated using WinMDI version 2.8 software. Data are expressed as mean $\pm$ S.D., $n = 5$.

complexes used. Particularly, the former could represent a more efficient ROS producer and the latter a more toxic and permeating compound. To evaluate the contribution of oxidative stress in the execution of apoptosis, we used SH-SY5Y cells transfected with an additional copy of the human superoxide dismutase 1 gene (*h*SOD cells) or differentiated by means of 7 days of incubation with 20 μM RA. Fig. 7*A* shows the results obtained by direct counts of dead cells after trypan blue staining, and demonstrates that *h*SOD cells were more resistant to both compounds than parental SH-SY5Y, even though to different extents. The increased antioxidant defense let *h*SOD cells be highly resistant to Cu(isapn)-induced cytotoxicity, whereas a moderate decrease in dead cells upon Cu(isaepy)$_2$ treatment was observed at 48 h. These results give support to a different mode of action of the two copper complexes, in which ROS production represents a crucial upstream event in apoptosis induced by Cu(isapn), but only plays a downstream additional role in Cu(isaepy)$_2$ cytotoxicity. The p53/p21 pathway was also activated upon both treatments, although with different kinetics. In fact, p53 and p21 seemed highly expressed after 6 and 12 h of treatments with Cu(isaepy)$_2$ and Cu(isapn), respectively; but no activation was observed after 24 h (Fig. 7*B*). These results suggest that Cu(isapn) and Cu(isaepy)$_2$ exert similar inhibitory effects on cell growth of parental SH-SY5Y and *h*SOD cells, a result confirmed by cell direct counts of attached viable cells (data not shown). To test whether such compounds functioned as nonspecific toxic agents, or were less efficient toward untransformed cells, we induced differentiation with prolonged RA incubations. The results obtained would have provided significant information about a potential approach for a selective use of copper complexes in cancer treatment. Seven days incubation with 20 μM RA conferred efficient protection against both copper complexes. A significant decrease of sub-G$_1$ cells to values close to untreated cells (about 4.25% after 48 h as shown in Fig. 7*C*) and no activation of the p53/p21 system was observed under these experimental conditions (Fig. 7*D*). The average 1-fold increase of SOD and catalase activity (data not shown), together with the inhibition of cell proliferation, features found in normal (untransformed) cells, are some of the modifications induced by RA incubation and may contribute to cell resistance against Cu(isapn)- and Cu(isaepy)$_2$-mediated toxicity.

Cu(isapn) and Cu(isaepy)$_2$-mediated Toxicity Is a Copper-mediated Event That Induces Nuclear and Mitochondrial Dysfunction—Cu(isapn) and Cu(isaepy)$_2$ are lipophilic compounds that may vehicle copper and allow the catalysis of redox reactions and ROS production to take place also within specific intracellular organelles. We evaluated the copper content in cellular fractions of SH-SY5Y cells (the purity of which is shown in supplemental data Fig. S2) treated for different times with the copper complexes. Fig. 8*A* shows atomic absorption analyses, which reveal a significant increase of copper in nuclear and mitochondrial fractions upon treatment with both compounds, with a trend mirroring total copper uptake and suggesting a likely copper-mediated site-directed injury. To evaluate the degree of the insult induced, we investigated if mitochondria and nuclei were damaged upon treatment with the two copper complexes. Fig. 8*B* shows SH-SY5Y nuclei stained with an antibody against the phospho-active histone H2A.X, which is phosphorylated on Ser^{139} after DNA double strand break. After 6 and 12 h of treatment, the appearance of discrete *foci*, indicating the recruiting sites of the DNA repair machinery, revealed DNA-specific damage mediated by Cu(isaepy)$_2$ and, to a lesser extent by Cu(isapn) treatment, a phenomenon that was further confirmed by Western blot analyses of nuclear fractions (Fig. 8*C*). Concomitantly, we incubated

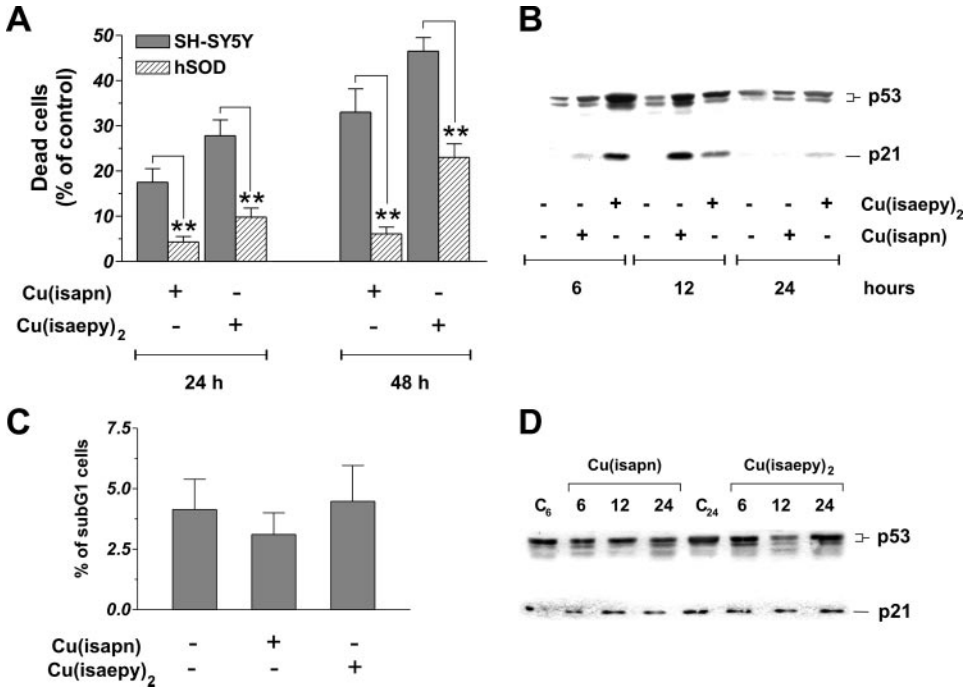

FIGURE 7. **The increase of antioxidant defense or differentiation by retinoic acid protects SH-SY5Y cells against Cu(isapn) and Cu(isaepy)$_2$-induced cytotoxic effects.** *A*, SH-SY5Y and *h*SOD cells were treated with 50 μM Cu(isapn) or Cu(isaepy)$_2$ for 24 and 48 h, adherent and floating cells were collected, washed with PBS, and counted upon trypan blue staining. Data are expressed as % of control and represent the mean ± S.D., $n = 6$; **, $p < 0.001$, with respect to parental cell line. *B*, *h*SOD cells were treated with 50 μM Cu(isapn) or Cu(isaepy)$_2$ for 6, 12, and 24 h. 25 μg of total protein extract was loaded onto each lane for detection of p53 and p21. Western blots are from one experiment representative of three that gave similar results. *C*, SH-SY5Y cells were incubated with 20 μM retinoic acid, to induce differentiation, then treated with 50 μM Cu(isapn) or Cu(isaepy)$_2$ for 24 h, washed, and stained with propidium iodide. Analysis of sub-G$_1$ (apoptotic) cells was performed by a FACScalibur instrument and percentages of staining positive cells were calculated using WinMDI version 2.8 software. Data are expressed as mean ± S.D., $n = 6$. *D*, SH-SY5Y cells were incubated with 20 μM retinoic acid, then treated with 50 μM Cu(isapn) or Cu(isaepy)$_2$ for 6, 12, and 24 h. 25 μg of total protein extract was loaded onto each lane for detection of p53 and p21. Western blots are from one experiment representative of three that gave similar results.

SH-SY5Y cells with MitoTracker Red, a red fluorescent dye that stains mitochondria in viable cells and that accumulates depending upon transmembrane potential ($\Delta\Psi_{mit}$). Fig. 8*D* shows that especially for Cu(isaepy)$_2$ treatment, a huge number of mitochondria resulted completely depolarized 12 h after treatment; $\Delta\Psi_{mit}$-dependent fluorescence was localized only in single spots and did not look like a continuous network as in untreated cells. These results give strength to the hypothesis that although Cu(isaepy)$_2$ does produce less ROS, it is more efficient than Cu(isapn) in inducing apoptosis, because of its ability to specifically accumulate and damage fundamental organelles, such as the nucleus and mitochondria.

To evaluate further the contribution of copper in Cu(isaepy)$_2$-induced apoptosis, we synthesized an analogous complex molecule in which zinc, a non-redox active metal ion, replaced copper in the complex. Alternatively, before Cu(isaepy)$_2$ administration, we incubated the cells with 150 μM of the non-permeating copper chelator TRIEN, which is able to remove copper from the complex and prevent its uptake by the cells. Cytofluorimetric analyses shown in Fig. 8*E* demonstrate that either upon treatment with Zn(isaepy) (Fig. 1*C*), or by preincubating the cells with TRIEN, the extent of sub-G$_1$ cell population strongly decreased with respect to Cu(isaepy)$_2$-treated cells, although a significant percentage of apoptosis was still detectable ($n = 6$, $p < 0.05$ with respect to untreated cells). These results suggest that copper plays a fundamental role in Cu(isaepy)$_2$-mediated apoptosis, presumably due to its action as catalyst of redox reactions; however, the isatin-Schiff base could also contribute to the toxicity observed.

Cu(isapn) and Cu(isaepy)$_2$ Induce Apoptosis via the Mitochondrial Pathway in Other Tumor Cell Types—Finally, to verify a general pro-apoptotic activity of the more efficient copper complex Cu(isaepy)$_2$, we selected two other human tumor cells, the promonocytoma U937 and the melanoma M14. As previously done with SH-SY5Y cells, we treated U937 and M14 cells with 50 μM Cu(isaepy)$_2$. Fig. 9*A* shows representative cytofluorimetric panels that demonstrate that treatment with this copper complex induced apoptosis after 24 h in both the tumor cell lines selected, with U937 cells being more susceptible. Western blot analyses of caspase-9, caspase-3, and PARP, performed at 24 and 48 h, further confirmed that the intrinsic mitochondrial pathway represents the preferential route for the induction of apoptosis (Fig. 9*B*). These results demonstrate the ability of Cu(isaepy)$_2$ in inducing cell death in different tumor cells, and suggest a general application of the molecule.

CONCLUSIONS

In this paper we report that two recent synthesized isatin-Schiff base copper(II) complexes Cu(isapn) and Cu(isaepy)$_2$ are able to induce apoptosis via the mitochondrial pathway in neuroblastoma SH-SY5Y cells and in other tumor histotypes, mainly by copper-dependent oxidative stress and nuclear/mitochondrial site-directed damage. Although both compounds are capable of producing such effects, the difference in the time of appearance of pro-apoptotic and oxidative markers and the extent of cell death depends on their efficiency to permeate the cell. Cu(isapn), although less permeating, seems more prone to produce oxyradicals and induce oxidative stress, whereas Cu(isaepy)$_2$ easily crosses cell membranes, accumulates, and damages nuclear and mitochondrial compartments at very early times. In line with these features, we speculate that the absence of a detectable "cytosolic" oxidative stress upon treatment with Cu(isaepy)$_2$ explain the absence of a critical redox activation of the JNK-mediated signaling cascade in the events leading to cell death.

Moreover, our data are equally supportive of parallel p53-dependent and -independent pathways, as demonstrated by experi-

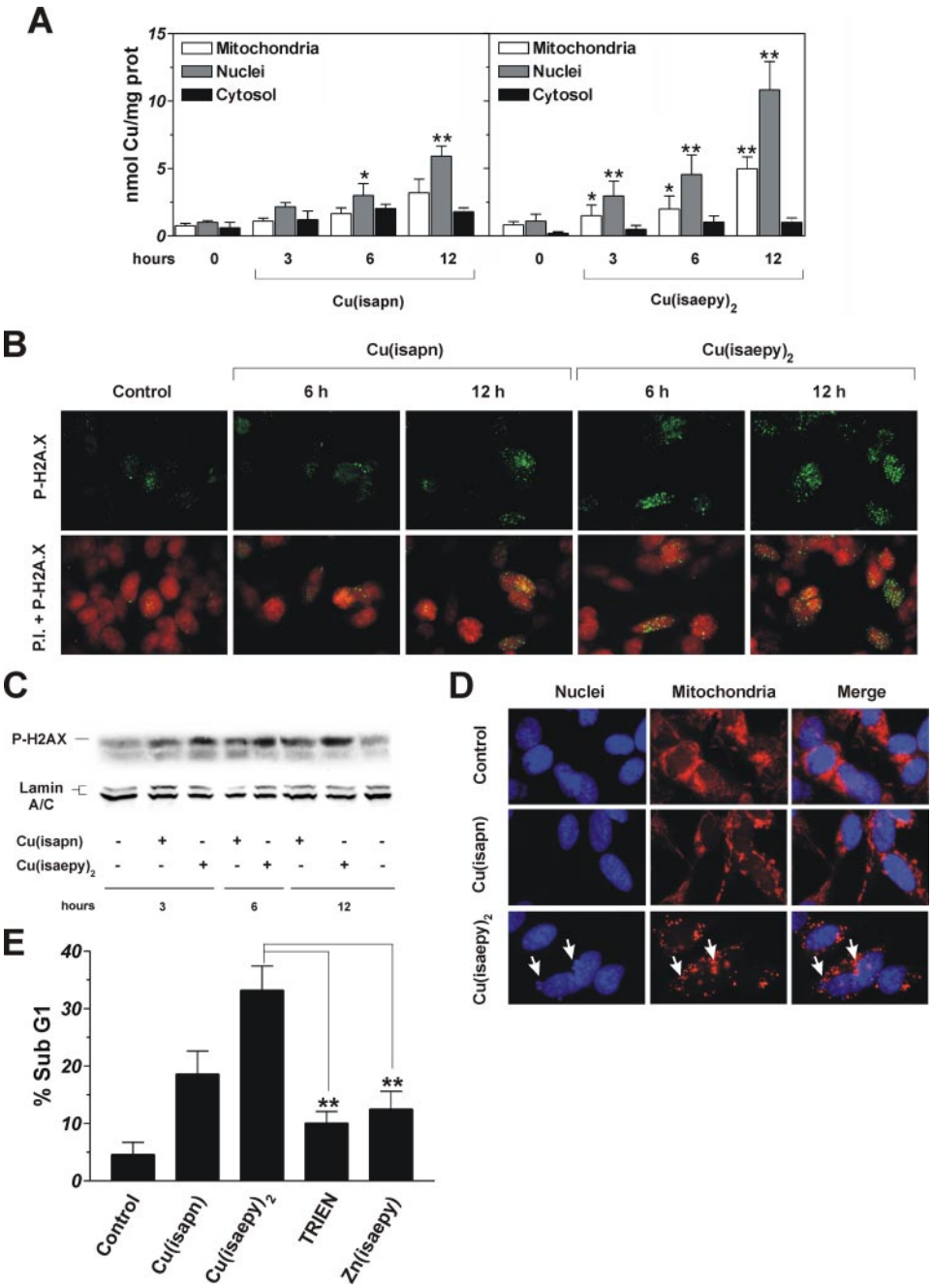

FIGURE 8. **Copper is fundamental in Cu(isapn) and Cu(isaepy)$_2$-induced apoptosis and is associated with the specific damage to nuclear and mitochondrial compartments.** *A*, SH-SY5Y cells were treated with 50 μM Cu(isapn) or Cu(isaepy)$_2$ for 3, 6, and 12 h, and exhaustively washed with PBS containing 1 mM EDTA to avoid contamination of extracellularly membrane-bound copper. Cells were then subjected to separation into nuclear, mitochondrial, and cytosolic enriched fractions, subsequently diluted 1:2 with 65% HNO_3, maintained at room temperature for 1 week, and analyzed by atomic absorption for copper content. Data are expressed as nanomole of copper/mg of total protein and represent the mean ± S.D., $n = 5$; *, $p < 0.05$; **, $p < 0.001$, with respect to cytosolic copper concentrations. *B*, SH-SY5Y cells were grown on chamber slides, treated for 6 and 12 h with 50 μM Cu(isapn) or Cu(isaepy)$_2$, and incubated with an anti-phospho-histone H2A.X antibody (*green*), to detect nuclear damage, and propidium iodide (*red*), to visualize nuclei. Images were digitized with a Cool Snap video camera connected to Nikon Eclipse TE200 fluorescence microscopy. *C*, alternatively, after 3, 6, and 12 h of treatment, nuclei of SH-SY5Y cells were isolated and lysed. 50 μg of total nuclear extract was loaded onto each lane and used for the detection of the phosphorylated form of histone H2A.X. Lamin A/C was used as nuclear loading control. *D*, SH-SY5Y cells were grown on chamber slides and treated for 12 h with 50 μM Cu(isapn) or Cu(isaepy)$_2$. Before fixation, cells were incubated for 30 min with 50 nM MitoTracker Red and subsequently stained with the specific nuclear vital dye Hoechst 33342. *White arrows* indicate the formation of nuclear fragment characteristic of cells undergoing apoptosis. Images were digitized with a Cool Snap video camera connected to Nikon Eclipse TE200 fluorescence microscopy. All of images were captured under constant exposure time, gain and offset. *E*, SH-SY5Y cells were treated with 50 μM Cu(isapn), Zn(isaepy), or 50 μM Cu(isaepy)$_2$ with or without the non-permeating copper chelator TRIEN (150 μM) for 24 h. Cells were then washed and stained with propidium iodide. Analysis of sub-G_1 (apoptotic) cells was performed by a FACScalibur instrument and percentages of staining positive cells were calculated using WinMDI version 2.8 software. Data are expressed as mean ± S.D., $n = 6$; **, $p < 0.001$, with respect to Cu(isaepy)$_2$-treated cells.

ments carried out in p53 knocked-down cells by siRNA or in cell lines lacking p53. These results are of great interest because functional p53 is frequently lost in human tumorigenesis.

The results obtained indicate that the role of copper in Cu(isapn) and Cu(isaepy)$_2$ cytotoxicity is fundamental, because of its capability to catalyze one-electron redox cycle reactions

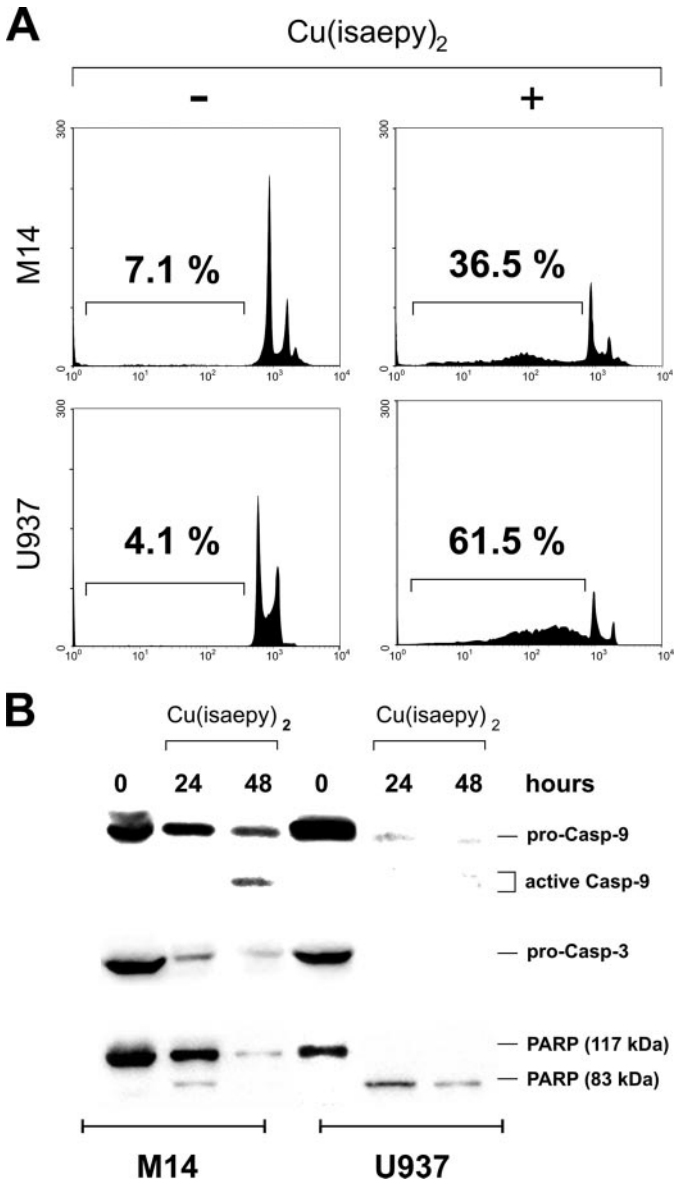

FIGURE 9. **Cu(isapn) and Cu(isaepy)$_2$ induce mitochondria-dependent apoptosis in U937 and M14 cells.** *A*, human melanoma M14 and promonocytoma U937 were treated with 50 μM Cu(isaepy)$_2$ for 24 h, washed, and stained with propidium iodide. Analysis of cell cycle and apoptosis was performed by a FACScalibur instrument and percentages of staining positive cells were calculated using WinMDI version 2.8 software. The cell cycle plots reported are from a typical experiment done in triplicate of five that gave similar results. The percentages of apoptotic nuclei are shown *above* each histogram. *B*, alternatively, M14 and U937 cells were treated with 50 μM Cu(isaepy)$_2$ for 24 and 48 h. 40 μg of total protein extract was loaded onto each lane for detection of pro- and active caspase-9, pro-caspase 3, and PARP. Western blots are from one experiment representative of three that gave similar results.

with oxygen thus producing ROS; the combination of this property with the chemical structure of the organic ligand binding the metal ion seems to give the specificity of the cellular damage induced. We suggest that the presence of copper is mainly required for nuclear damage, similar to what iron does in the presence of bleomycin (37, 38), whereas the isatin-imine ligand is important to carry the redox-active metal ion across cellular membranes, and could be more active at the mitochondrial level. This hypothesis is strengthened by the similarity of the chemical structure of Cu(isapn) and Cu(isaepy)$_2$ with the delocalized lipophilic cations, a class of molecules able to permeate the cell in response to negative transmembrane potentials and increase their concentration, particularly into mitochondria (39). The higher plasma and mitochondrial membrane potentials of tumor cells compared with normal cells account for the preferential accumulation of delocalized lipophilic cations in carcinoma mitochondria (40, 41). Because most delocalized lipophilic cations are toxic to mitochondria at high concentrations, their selective accumulation in the mitochondria of tumor cells, and consequent mitochondrial toxicity, provide the basis for selective tumor cell killing. The capability of this compound to preferentially induce detrimental effects in transformed cells can also be suggested on the basis of the preliminary results obtained in the presence of RA, which is able to protect the cells by making them similar to differentiated lines.

Overall, the results obtained allow us to suggest a dual role for Cu(isapn) and Cu(isaepy)$_2$ in the induction of apoptosis: on one hand they are able to vehicle copper into the cell, thus producing ROS; on the other they could behave as delocalized lipophilic cations, thus specifically targeting mitochondria. Therefore the chemical structure of the isatin-Shiff base represents the "switch" between these properties. This suggests that by specifically changing the chemical characteristics of this ligand type, we may modulate the cytotoxic effects induced, thus exploiting the plasticity of this new class of compounds to improve the therapeutic selectivity to different tumor histotypes.

REFERENCES

1. Blagosklonny, M. V., and Pardee, A. B. (2001) *Cancer Res.* **61,** 4301–4305
2. Shapiro, G. I. (2006) *J. Clin. Oncol.* **24,** 1770–1783
3. Townsend, D. M., Findlay, V. L., and Tew, K. D. (2005) *Methods Enzymol.* **401,** 287–307
4. Kalinowski, D. S., and Richardson, D. R. (2005) *Pharmacol. Rev.* **57,** 547–583
5. Lyko, F., and Brown, R. (2005) *J. Natl. Cancer Inst.* **97,** 1498–1506
6. Wilson, L., and Jordan, M. A. (2004) *J. Chemother.* **16,** Suppl. 4, 83–85
7. Gius, D., and Spitz, D. R. (2006) *Antioxid. Redox. Signal.* **8,** 1249–1252
8. Griguer, C. E., Oliva, C. R., Kelley, E. E., Giles, G. I., Lancaster, J. R., Jr., and Gillespie, G. Y. (2006) *Cancer Res.* **66,** 2257–2263
9. Martin, V., Herrera, F., Carrera-Gonzalez, P., Garcia-Santos, G., Antolin, I., Rodriguez-Blanco, J., and Rodriguez, C. (2006) *Cancer Res.* **66,** 1081–1088
10. Prusty, B. K., and Das, B. C. (2005) *Int. J. Cancer* **113,** 951–960
11. Na, H. K., and Surh, Y. J. (2006) *Mol. Carcinog.* **45,** 368–380
12. Biaglow, J. E., and Miller, R. A. (2005) *Cancer Biol. Ther.* **4,** 6–13
13. Engel, R. H., and Evens, A. M. (2006) *Front. Biosci.* **11,** 300–312
14. Cleveland, J. L., and Kastan, M. B. (2000) *Nature* **407,** 390–395
15. Miller, R. A., Woodburn, K. W., Fan, Q., Lee, I., Miles, D., Duran, G., Sikic, B., and Magda, D. (2001) *Clin. Cancer Res.* **7,** 3215–3221
16. Gewirtz, D. A. (1999) *Biochem. Pharmacol.* **57,** 727–741
17. Kotamraju, S., Kalivendi, S. V., Konorev, E., Chitambar, C. R., Joseph, J., and Kalyanaraman, B. (2004) *Methods Enzymol.* **378,** 362–382
18. Daniel, K. G., Gupta, P., Harbach, R. H., Guida, W. C., and Dou, Q. P. (2004) *Biochem. Pharmacol.* **67,** 1139–1151
19. Chen, D., Peng, F., Cui, Q. C., Daniel, K. G., Orlu, S., Liu, J., and Dou, Q. P. (2005) *Front. Biosci.* **10,** 2932–2939
20. Gaetke, L. M., and Chow, C. K. (2003) *Toxicology* **189,** 147–163
21. Rossi, L., Aquilano, K., Filomeni, G., Lombardo, M. F., Rotilio, G., and Ciriolo, M. R. (2004) in *Frontiers in Neurodegenerative Disorders and Aging: Fundamental Aspects, Clinical Perspectives and New Insights* (Ozben, K., and Chevion, M., eds) pp. 207–250, IOS Press, Amsterdam
22. Filomeni, G., Rotilio, G., and Ciriolo, M. R. (2005) *Cell Death Differ.* **12,**

1555–1563
23. Radulovic, S., Tesic, Z., and Manic, S. (2002) *Curr. Med. Chem.* **9,** 1611–1618
24. Katsaros, N., and Anagnostopoulou, A. (2002) *Crit. Rev. Oncol. Hematol.* **42,** 297–308
25. Rosenzweig, A. C. (2001) *Acc. Chem. Res.* **34,** 119–128
26. Wang, T., and Guo, Z. (2006) *Curr. Med. Chem.* **13,** 525–537
27. Saryan, L. A., Ankel, E., Krishnamurti, C., Petering, D. H., and Elford, H. (1979) *J. Med. Chem.* **22,** 1218–1221
28. Antholine, W. E., Knight, J. M., and Petering, D. H. (1976) *J. Med. Chem.* **19,** 339–341
29. Cerchiaro, G., Aquilano, K., Filomeni, G., Rotilio, G., Ciriolo, M. R., and Ferriera, A. M. D. C. (2005) *J. Inorg. Biochem.* **99,** 1433–1440
30. Cerchiaro, G., Micke, G. A., Tavares, M. F. M., and Ferriera, A. M. D. C. (2004) *J. Mol. Catalysis A Chem.* **221,** 29–39
31. Ciriolo, M. R., De Martino, A., Lafavia, E., Rossi, L., Carri, M. T., and Rotilio, G. (2000) *J. Biol. Chem.* **275,** 5065–5072
32. Nicoletti, I., Migliorati, G., Pagliacci, M. C., Grignani, F., and Riccardi, C. (1991) *J. Immunol. Methods* **139,** 271–279
33. Filomeni, G., Aquilano, K., Rotilio, G., and Ciriolo, M. R. (2005) *Antioxid. Redox. Signal.* **7,** 446–455
34. Filomeni, G., Rotilio, G., and Ciriolo, M. R. (2003) *FASEB J.* **17,** 64–66
35. Filomeni, G., Aquilano, K., Rotilio, G., and Ciriolo, M. R. (2003) *Cancer Res.* **63,** 5940–5949
36. Lowry, O. H., Rosebrough, N. J., Farr, A. L., and Randall, R. J. (1951) *J. Biol. Chem.* **193,** 265–275
37. Ciriolo, M. R., Peisach, J., and Magliozzo, R. S. (1989) *J. Biol. Chem.* **264,** 1443–1449
38. Harsch, A., Marzilli, L. A., Bunt, R. C., Stubbe, J., and Vouros, P. (2000) *Nucleic Acids Res.* **28,** 1978–1985
39. Modica-Napolitano, J. S., and Aprille, J. R. (2001) *Adv. Drug Deliv. Rev.* **49,** 63–70
40. Davis, S., Weiss, M. J., Wong, J. R., Lampidis, T. J., and Chen, L. B. (1985) *J. Biol. Chem.* **260,** 13844–13850
41. Modica-Napolitano, J. S., and Aprille, J. R. (1987) *Cancer Res.* **47,** 4361–4365